Rigorous Analysis of the Scattering of Surface Waves in an Abruptly Ended Slab Dielectric Waveguide

PHILIPPE GELIN, MICHEL PETENZI, AND JACQUES CITERNE

Abstract—**The reflection and the scattering properties of even TE and TM surface waves incident in an abruptly ended dielectric slab waveguide are analyzed. The discontinuity is regarded as a junction between two open waveguides namely the dielectric slab waveguide and the free space waveguide. The boundary conditions acting together with the orthogonality provide singular coupled integral equations on the discrete and the continuous wave amplitudes at the discontinuity. These singular coupled integral equations with Cauchy kernels and infinite limits of integration are solved by iteration via the Neuman series. Numerical results are presented for the reflectivity of the even TE_0 and TM_0 fundamental modes, together with their mode conversion on even TE_2 and TM_2 in a slab where two guided modes can propagate. Reflectivity and mode conversion of higher order excitations are also investigated.**

I. Introduction

THE DIFFICULTY of the studies relating to open waveguide discontinuities led many authors to concentrate on rather elementary problems of dielectric slab waveguide. Such problems are idealization of more realistic situations that occur at a transverse discontinuity in a planar waveguide in centimeter, millimeter, or optical circuitry design.

We would have wished here to formulate rigorously the resonant conditions of confined modes inside a lossless dielectric resonator [1], however, owing to the complexity of this problem which remains unsolved up to date, to our knowledge, we shall consider in the present paper transverse discontinuities in dielectric slabs, rather than in circular dielectric rods.

The methods outlined in pioneer works on abrupt junctions between one surface waves guiding structure to another are, in essence, similar to those used for junctions between more conventional closed waveguides [2]. They are to be adapted to treat open structures where the complete set of eigenmodes includes both discrete and continuous waves.

Most of the theoretical analyses reported previously were restricted to small discontinuities. Under that basic assumption, either the backward radiated waves can be neglected as in [3] or the continuum keeps the same description on both sides of the discontinuity as in [4]. The problem of arbitrarily large steps under monomode or multimode excitations has been also investigated by several authors. For computational convenience, Mahmoud and Beal [5] transformed the continuous description of the radiation modes in a discrete one by expanding the coupling functions in terms of a complete set of normalized Laguerre polynomials on the range of the continuous transverse wavenumber. Very recently, two variational approaches have been applied successfully. Using the aforementioned discrete description of the continuum, Morishita *et al.* [6] defined the mean square error of the transverse fields components at the discontinuity as a functional and solved the stationary associated boundary value problem. Rozzi [7] solved the integral equation given in [8] on the transverse fields components at the discontinuity interface via the Ritz–Galerkin method; the normalized Laguerre polynomials are still used but for discretizing the modal fields components in each slab waveguide cross section.

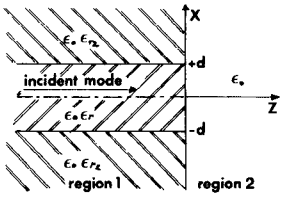

Fig. 1. Abruptly ended dielectric slab waveguide configuration.

This paper deals with an other rigorous approach of the surface wave scattering at a transverse discontinuity in a lossless dielectric slab waveguide. It consists of deriving coupled singular integral equations on discrete and continuous wave amplitudes interfering in the total electromagnetic fields which are matched at the discontinuity interface. This system of singular integral equations, where the integrals are taken in the sense of the Cauchy principal values, is solved by interation using the standard Neuman series which are found rapidly converging.

The method has already been succinctly described elsewhere for arbitrarily large steps [9] but without computational details. In the present paper, we are going to discuss an open-type discontinuity problem of great interest in resonator design, i.e., the diffraction and the reflection of surface waves at abruptly ended slab dielectric waveguide (Fig. 1).

Such a problem is also of great importance in other area of activity such as in solid-state heterojunction laser devices [10] and in millimeter wave antenna applications

Manuscript received October 23, 1979; revised September 26, 1980.

The authors are with the Propagation and Circuits Group, Microwave and Semiconductor Center, LA CNRS no. 287, Technical University of Lille, 59655, Villeneuve D'Ascq Cedex, France.

0018-9480/81/0200-0107$00.75 ©1981 IEEE

[11]. For a laser cavity, the reflection and the diffraction of surface waves at the end facet are crucial parameters for determining both its oscillation condition and its output coupling radiation in free space. For dielectric slab antennas, the usual parameters are the terminal impedance and the near as well as far scattered fields.

The problem we discuss in this paper has thus already been investigated in the aforementioned areas by several authors who proposed numerical results under reasonable approximations. Most of them used the transverse integral equation method associated with a final variational formulation on quantities which have a stationary property. These quantities are the terminal and transfert impedances in [12] and [13] whereas in [14] and in [15] they are the reflection coefficients. This paper can be considered as extension of Rozzi works recently published [16].

The technique we are going to describe gives an exact solution of this basic problem and the computational effort required is minimum. For brevity's sake, it will be restricted to even TE excitations. The TM excitations is briefly treated in Appendix.

II. Analysis of the Abruptly Ended Slab Discontinuity

A. Formulation of the Problem

On the left-hand side of the interface discontinuity $z=0$, the discrete and the continuous parts of the spectrum of the slab dielectric waveguide are derived using Marcuse notations [3]. On the right-hand side of the interface $z=0$, the spectrum is only continuous; its description is deduced from the slab continuous spectrum by taking the limit of either a zero thickness ($d\to 0$) or a unit permittivity ($\epsilon_r \to 1$). For simplicity only the even TE waves with transverse fields E_y and H_x are considered. Continuity of these transverse fields at the interface $z=0$ is expressed as

$$\begin{Bmatrix} E^i_{y,0} \\ H^i_{x,0} \end{Bmatrix} + \sum_n a_n \begin{Bmatrix} E^r_{y,n} \\ H^r_{x,n} \end{Bmatrix} + \int_0^\infty q^r(\rho) \begin{Bmatrix} E^r_y(\rho) \\ H^r_x(\rho) \end{Bmatrix} d\rho = \int_0^\infty q^t(\rho) \begin{Bmatrix} E^t_y(\rho) \\ H^t_x(\rho) \end{Bmatrix} d\rho, \qquad n=0,2,4,\cdots. \quad (1)$$

The field on the left-hand side of (1) is a superposition of the even incident TE_0 mode (superscript i), of the reflected even discrete TE_n ($n=0,2,4,\cdots$) and of the reflected even continuous TE modes (superscript r). The constants a_n ($n=0,2,4,\cdots$) are the amplitudes of the reflected discrete modes, while the coefficients $q^r(\rho)$ represent the amplitudes of the reflected continuous modes. The forward scattered field on the right-hand side of (1) is a superposition of the transmitted even TE continuous modes with the amplitudes $q^t(\rho)$. In the following, we denote by β_n ($n=0,2,4,\cdots$) and $\beta(\rho)$ the phase constant of the even discrete TE_n modes and of the even continuous TE modes, respectively; lastly, ρ denotes the transverse wavenumber of the slab continuous modes outside the dielectric medium.

By using orthogonality and by operating elementary substitutions, we can take out from (1), the amplitudes $q^t(\rho)$, a_n and $q^r(\rho)$, the expressions of which are

$$q^t(\rho) = \frac{1}{\omega\mu_0 P} \frac{|\beta(\rho)|}{[\beta_0+\beta(\rho)]} \left\{ 2\beta_0 \int_0^\infty E^i_{y,0} \cdot E^t_y(\rho) \cdot dx + \int_0^\infty d\rho' \int_0^\infty q^r(\rho') \cdot [\beta_0 - \beta(\rho')] \cdot E^r_y(\rho') \cdot E^t_y(\rho)\, dx + \sum (\beta_0 - \beta_n) \cdot a_n \int_0^\infty E^r_{y,n} E^t_y(\rho)\, dx \right\}, \qquad n=2,4,\cdots \quad (2)$$

$$\begin{Bmatrix} a_n \\ q^r(\rho) \end{Bmatrix} = \frac{1}{2\omega\mu_0 P} \cdot \frac{\begin{Bmatrix} \beta_n \\ |\beta(\rho)| \end{Bmatrix}}{\begin{Bmatrix} \beta_n \\ \beta(\rho) \end{Bmatrix}} \cdot \int_0^\infty d\rho' \int_0^\infty q^t(\rho') \left[\begin{Bmatrix} \beta_n \\ \beta(\rho) \end{Bmatrix} - \beta(\rho') \right] \cdot E^t_y(\rho') \cdot \begin{Bmatrix} E^r_{y,n} \\ E^r_y(\rho) \end{Bmatrix} dx, \qquad n=0,2,4,\cdots \quad (3)$$

where P is the real power flow in the positive z direction (per unit length of y) for any discrete propagating mode. The continuous modes, which can be either propagating or evanescent have their complex power flow $\mathcal{P}$ related to P by the following formula:

$$\mathcal{P} = \frac{\beta(\rho)}{|\beta(\rho)|} P. \quad (4)$$

Equations (2) and (3) are the coupled integral equations that relate the unknown functions $q^t(\rho)$, a_n, and $q^r(\rho)$. These equations have to be solved for treating rigorously the abruptly ended dielectric slab discontinuity problem. Beside the unknown functions $q^t(\rho)$, a_n, and $q^r(\rho)$, all other quantities in (2) and (3) are known since they refer to the slab and to the free space TE modal fields.

B. Closed Form of the Coupled Integral Equations

Using the analytical expressions of slab and free space TE modal fields components (see [3]), we can give below the closed form of the coupled integral (2) and (3)

$$q^t(\rho) = \frac{1}{2\omega\mu_0 P} \frac{|\beta(\rho)}{[\beta_0+\beta(\rho)]} \cdot \left\{ 2\beta_0 \cdot G_0(\rho) + \int_0^\infty q^r(\rho')[\beta_0 - \beta(\rho')] \cdot F(\rho', \rho)\, d\rho' + \sum (\beta_0 - \beta_n) \cdot a_n \cdot G_n(\rho) \right\}, \qquad n=2,4,\cdots \quad (5)$$

$$\begin{Bmatrix} a_n \\ q^r(\rho) \end{Bmatrix} = \frac{1}{4\omega\mu_0 P} \frac{\begin{Bmatrix} \beta_n \\ |\beta(\rho)| \end{Bmatrix}}{\begin{Bmatrix} \beta_n \\ \beta(\rho) \end{Bmatrix}} \cdot \int_0^\infty q^t(\rho') \cdot \left[\begin{Bmatrix} \beta_n \\ \beta(\rho) \end{Bmatrix} - \beta(\rho') \right] \cdot \begin{Bmatrix} G_n(\rho') \\ F(\rho, \rho') \end{Bmatrix} d\rho', \qquad n=0,2,4,\cdots \quad (6)$$

where

$$G_n(\rho)=2k_0^2(\epsilon_r-1)\cdot A_n\cdot B_e^t(\rho)\cos K_n d \cdot\frac{(\gamma_n\cos\rho d-\rho\sin\rho d)}{(K_n^2-\rho^2)(\gamma_n^2+\rho^2)} \quad (7)$$

$$F(\rho',\rho)=\Pi B_e^t(\rho)B_e^r(\rho')\left[D_e^r(\rho')+D_e^{r*}(\rho')\right]\delta(\rho-\rho') -k_0^2(\epsilon_r-1)B_e^t(\rho)B_e^r(\rho') \cdot\left[\frac{\sin(\sigma'+\rho)d}{\sigma+\rho}+\frac{\sin(\sigma'-\rho)}{\sigma'-\rho}\right]\frac{1}{\rho'^2-\rho^2} \quad (8)$$

where A_n, $B_e^r(\rho)$, $D_e^r(\rho)$, and $B_e^t(\rho)$ are the normalized amplitudes of the even guided and continuous TE modes in each regions. Their analytical expressions are still available in [3].

In order to test the validity of the solution of the coupled integral equation system, (5) and (6), an additional integral equation between the unknown functions can be derived from (1), namely

$$(1+a_0)(1-a_0^*)=\sum|a_n|^2+\int_0^\infty(|q^t(\rho)|2 +|q^r(\rho)|^2)\frac{\beta^*(\rho)}{|\beta(\rho)|}d\rho, \qquad n=2,4,\cdots. \quad (9)$$

This relation can be split into its real and its imaginary parts. The former gives the law of power conservation at the discontinuity

$$1-\sum|a_n|^2=\int_0^{k_0}\left[|q^t(\rho)|^2+|q^r(\rho)|^2\right]d\rho, \qquad n=0,2,4,\cdots \quad (10)$$

while the latter is the imaginary part of the a_0 reflection coefficient which is expressed as

$$\mathrm{Im}(a_0)=\frac{1}{2}\int_{k_0}^\infty\left[|q^t(\rho)|^2+|q^r(\rho)|^2\right]d\rho. \quad (11)$$

Equations (10) and (11) may be used to measure the power coupled on the radiated modes and the energy stored by the evanescent modes. Owing to the fact that the modulus of the reflection coefficient is bounded ($\mathrm{Im}(a_0)<1$), the continuous wave amplitudes are necessarily decreasing faster than $\rho^{-1/2}$ as $\rho\to\infty$. By inserting the expression (8) of the function $F(\rho',\rho)$ into the $q^t(\rho)$ and $q^r(\rho)$ integral equations (5) and (6), a singularity of the Cauchy type appears in each kernel at $\rho=\rho'$. Expressing each kernel in a generalized form $H(\rho',\rho)/(\rho'-\rho)$ where the function $H(\rho',\rho)$ is bounded everywhere, it becomes obvious that considering the Cauchy principle value of the integrals, or assuming that near $\rho=\rho'$

$$\lim_{\epsilon\to0}\int_{\rho-\epsilon}^{\rho+\epsilon}q^t(\rho')\frac{H(\rho',\rho)}{\rho'-\rho}d\rho'=0 \quad (12)$$

are identical conditions. Equation (12) means that near $\rho=\rho'$ the bounded function $q^t(\rho)\cdot H(\rho',\rho)$ is slowly varying compared to the rapid variation of the unbounded quantity $1/(\rho'-\rho)$.

Using the Cauchy principle value of each integral, our numerical results indicate that the unknown functions

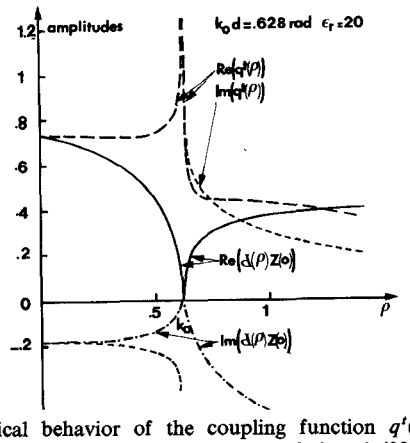

Fig. 2. Typical behavior of the coupling function $q^t(\rho)$ and $d(\rho)$ versus the transverse wavenumber ρ ($\epsilon_r=20$, $k_0=0.628$ rad/cm, $d=1$ cm).

$q^t(\rho)$ and $q^r(\rho)$ exhibit weak singularities at $\rho=k_0$. An illustration of the behavior of $q^t(\rho)$ versus the transverse wavenumber ρ is given in Fig. 2. Such observations have been already made by Rulf [17] who solved asymptotically a similar problem for the case of a small discontinuity. Although formally integrable, the singularity of $q^t(\rho)$ (or $q^r(\rho)$) can be described more accurately by changing variable as in [7]. The change of variable consist to include the modal characteristic impedance $Z(\rho)$ in continuity relations (1) in order to write

$$q\left\{{r\atop t}\right\}(\rho)=\left\{{b(\rho)\atop d(\rho)}\right\}\cdot Z(\rho), \qquad Z(\rho)=\alpha\cdot\frac{\omega\mu_0}{|\beta(\rho)|}$$

where $\alpha=1$ for $\rho\leqslant k_0$ and, $\alpha=j$ for $\rho\geqslant k_0$. The singularity appears clearly in the expression of $Z(\rho)$, whereas the functions $b(\rho)$ and $d(\rho)$ are now bounded as shown in Fig. 2.

A straightforward approach for solving the coupled integral equation system is achieved by means of an iterative procedure involving a series of approximations on the scattering mechanism. A first-order solution $[q^t(\rho)]_1$ is derived by neglecting the reflected discrete and continuous modes. We write

$$\left[q^t(\rho)\right]_1=\frac{1}{2\omega\mu_0P}\frac{|\beta(\rho)|}{\left[\beta_0+\beta(\rho)\right]}\cdot2\beta_0\cdot G_0(\rho). \quad (13)$$

Then we substitute $[q^t(\rho)]_1$ in the other integral equations to calculate the first-order solutions for $q^r(\rho)$ and a_n, which we note as $[q^r(\rho)]_1$ and $[a_n]_1$, respectively. Second-order solutions $[q^t(\rho)]_2$, $[q^r(\rho)]_2$, and $[a_n]_2$ are deduced using the previous first-order values of the waves amplitudes, and so on. This method is known as the Neuman series of the system of coupled integral equation [19].

The iterative scheme is terminated when the modulus of the difference between two successive orders of approximation for a_n ($n=0,2,4,\cdots$) is lower than some specified accuracy. At the last iteration, power conservation, (10), is checked.

III. Numerical Results

The numerical study has been carried out for both the TE and TM cases. In the former case we consider incident even modes TE_0 and TE_2 while in the latter case the

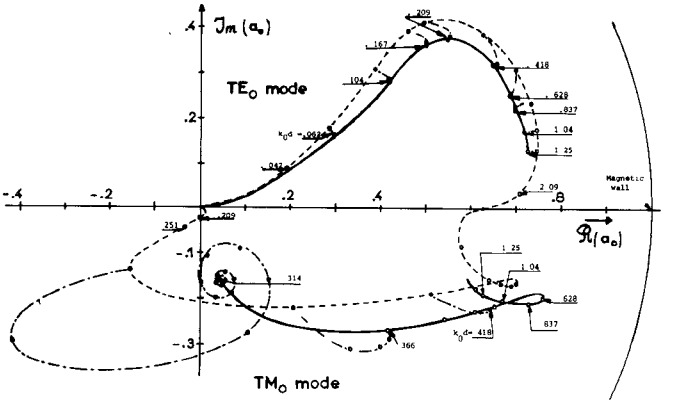

Fig. 3. Behavior of the reflection coefficient a_0 in the complex plane. ----- first-order approximation for a_0 versus k_0d. —·— convergence of a_0 versus the successive orders of approximation. —— exact solution for a_0 versus k_0d.

TABLE I

	TE_0 case; $\epsilon_r=20$					TM_0 case; $\epsilon_r=20$			
	(6)		(10)	(14)		(A-13)		(10)	(A-14)
k_0d	a_0	$\lvert a_0\rvert^2$	$\lvert a_0\rvert^2$	1	k_0d	a_0	$\lvert a_0\rvert^2$	$\lvert a_0\rvert^2$	1
0.209	$0.547+j.361$	0.435	0.435	0.997	0.314	$0.046-j.159$	0.027	0.026	$0.999-j.001$
0.418	$0.648+j.315$	0.519	0.520	0.997	0.418	$0.655-j.215$	0.476	0.486	0.999
0.628	$0.681+j.244$	0.523	0.524	0.997	0.628	$0.763-j.197$	0.622	0.628	$0.999+j.001$
0.837	$0.696+j.217$	0.531	0.531	0.999	0.837	$0.727-j.209$	0.572	0.580	$0.998+j.002$
1.04	$0.719+j.168$	0.545	0.544	0.999	1.04	$0.669-j.204$	0.486	0.475	$0.997-j.001$
1.25	$0.724+j.127$	0.540	0.540	0.999	1.25	$0.628-j.191$	0.431	0.444	0.999

incident even modes TM_0 and TM_2 are considered. The wave amplitudes are plotted against the normalized frequency k_0d with the relative slab permittivity as a parameter. High values for the permittivity are relevant for microwave dielectric resonators.

First it is necessary to test the convergence of the outlined method. The two reflection coefficients a_0 of the even TE_0 and TM_0 incident mode versus the successive orders of approximation are plotted in a complex-plane representation in Fig. 3. In Fig. 3 are sketched for a_0 1) the exact results, 2) the initial first-order results, and 3) the loci of successive orders of approximation of the iterative procedure. In the TE case, the convergence is very fast since four iterations only are needed for an accuracy better than 10^{-3}. Convergence in the TM case is quite different specially in the low-frequency region where it is very slow. In this low-frequency region, the phase constant of the discrete TM_0 guided mode β_0 reaches values close to the free space wavenumber k_0 and a very strong coupling with the reflected and transmitted continuous waves occurs. As an example for $k_0d=0.314$ about 15 iterations are needed for obtaining exact results inside a precision of 10^{-3}. The TM convergence appears quite similar to the TE convergence in the high-frequency region, and the first-order iterative solution is a good representation of the exact reflection coefficient a_0.

Accuracy of the computed results is illustrated by Table I. The square of the modulus of the reflection coefficient a_0 for both the TE_0 and the TM_0 incident modes are deduced either from the complex solution of the integral equations (5) and (6) for the TE case, and (A-12) and (A-13) for the TM case or directly from the power conservation integral equation (10). It can be noted that within a given precision of 10^{-3} in the iterative scheme which provides the value of a_0, power conservation is verified more accurately than 0.2 percent for the TE case and 1 percent for the TM case. In addition to (2) and (3), an other test on the accuracy of the value of the coupling coefficient $q^t(\rho)$ in the TE case can be carried out from the following relation:

$$1=\frac{1}{4\omega\mu_0 P}\int_0^\infty q^t(\rho)\cdot(\beta_0+\beta(\rho))\cdot G_0(\rho)\,d\rho \qquad (14)$$

which can be easily deduced from (1) using orthogonality. Due to the similarity between (14) and (6), which gives a_0, it is expected that the accuracy of 0.3 percent observed on the value of one (Table I) can be also used for the value of a_0. For the TM case, (A-14) takes place instead of (14). Numerically, a similar behavior of the convergence and accuracy has been found for the coupling coefficient a_2 in the range of variation of the normalized frequency which does not exceed the "cutoff frequency" of the third discrete mode in the slab when $\epsilon_r=20$. In a first paper [9] we have compared our results with those of Rozzi [7] for the step discontinuity; the agreement between the two analysis is quite good.

A second comparison with Ikegami's results is shown in Fig. 4. This figure presents the evolution of the power reflection coefficient of the facet of dh laser cavity versus the thickness of the active layer for two surrounding

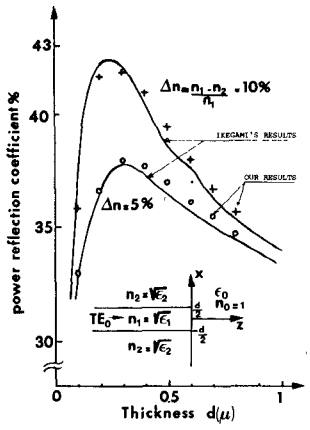

Fig. 4. Reflectivity of the TE_0 incident made at end facet of a dh laser cavity versus the thickness of the active layer.

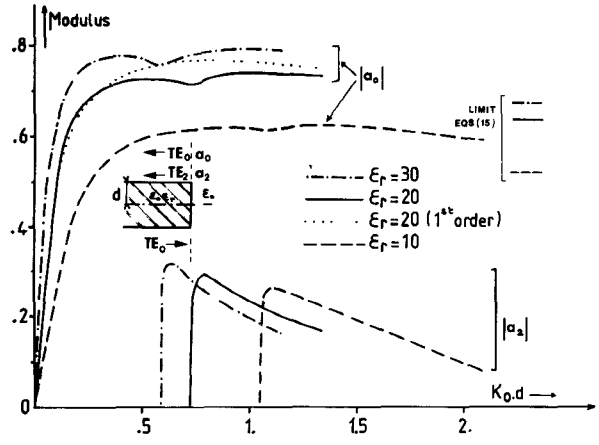

Fig. 5. Moduli of the reflection coefficient a_0 and of the coupling coefficient a_2 (incident TE_0 mode).

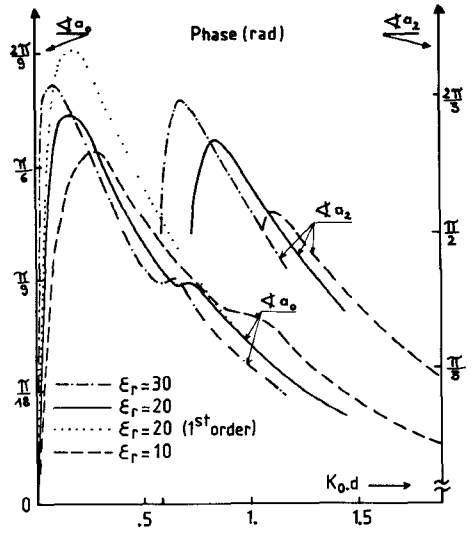

Fig. 6. Phases of the reflection coefficient a_0 and of the coupling coefficient a_2 (incident TE_0 mode).

materials with different index. Our results agree quite well with those of Ikegami [14].

Considering the even TE_0 mode incident in the semi-infinite dielectric slab, Figs. 5 and 6 illustrate the variations of the moduli and those of the phases of the reflection coefficient a_0 together with the coupling coefficient a_2 versus the normalized frequency k_0d. Similar curves now referring to TM_0 incident modes are plotted in Figs. 7 and 8. In Figs. 5 and 6 we note an irregularity in the behavior of the modulus and the phase of the a_0 reflection coefficient of the TE_0 incident mode as a function of k_0d which corresponds to the excitation of the TE_2 reflected mode in the slab waveguide. For the TM_0 incident mode, this irregularity does not appear in the behavior of the modulus of the reflection coefficient a_0 in Fig. 7 but it is noticeable in the phase curve of Fig. 8.

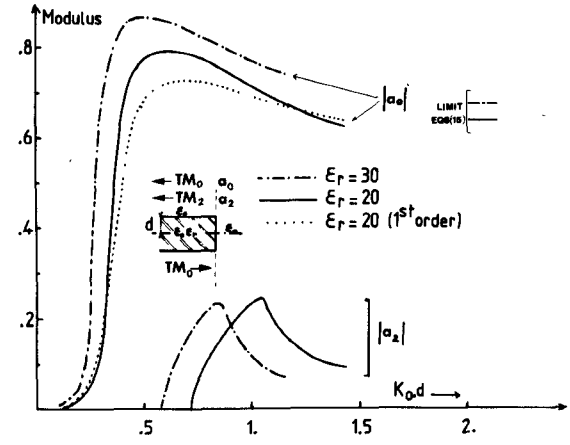

Fig. 7. Moduli of the reflection coefficient a_0 and of the coupling coefficient a_2 (incident TM_0 mode).

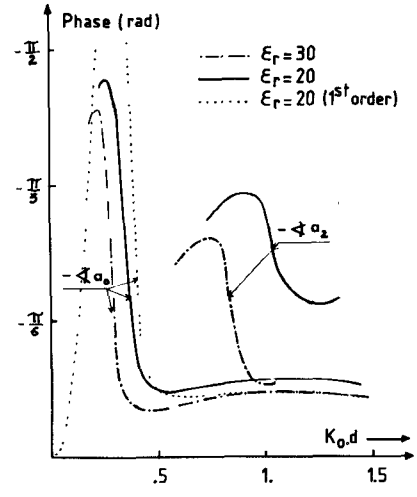

Fig. 8. Phases of the reflection coefficient a_0 and of the coupling coefficient a_2 (incident TM_0 mode).

As the normalized frequency increases, the reflection coefficients a_0 with both TE_0 and TM_0 excitations become virtually identical and their common value can be closely approximated by the reflection coefficient of a plane wave incoming from the higher index semi-infinite medium. This limiting value expressed as

$$a_0 = \frac{\sqrt{\epsilon_r} - 1}{\sqrt{\epsilon_r} + 1} \tag{15}$$

is drawn in Figs. 5 and 7 for all given values of the relative permittivity for the dielectric slab. Note also that the first-order approximations which agree with the exact

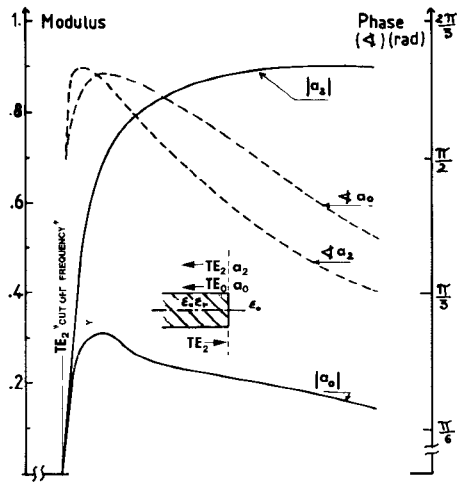

Fig. 9. Moduli (——) and phases (----) of the reflection coefficient a_2 and of the coupling coefficient a_0 (incident TE_2 mode, $\epsilon_r = 20$).

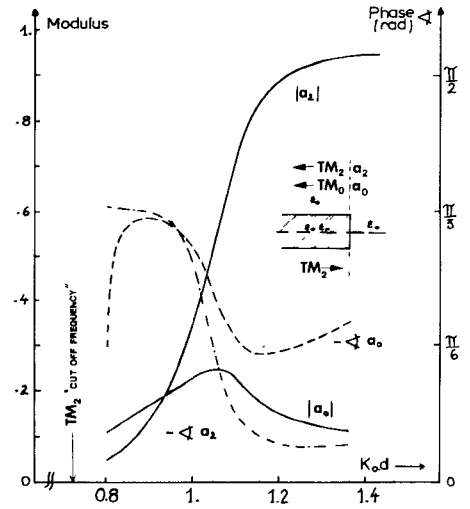

Fig. 10. Moduli (——) and phases (----) of the reflection coefficient a_2 and of the coupling coefficient a_0 (incident TM_2 mode, $\epsilon_r = 20$).

results as the normalized frequency is arising, tend toward the above limit value (15) of the reflection coefficient (see Fig. 3).

We continue the comparison between the behavior of the TE_0 and TM_0 excitation by noticing that the modulus of the reflection coefficient of the latter remains quite negligible in a large range of variation of low normalized frequencies. This feature corresponds to an important leakage of the energy by coupling with the radiative continuous modes at the discontinuity. In the TE case, the power coupled on the radiated modes decreases whereas the stored energy increases (see (10) and (11) and Fig. 3). This process is very fast after the cutoff frequency. Similar effect are felt by the coupling coefficient a_n $(n=2,4,\cdots)$ in the neighborhood of the "cutoff frequencies" of the higher order slab modes.

In Figs. 9 and 10 we use higher order mode excitations of the infinite dielectric slab, namely the even TE_2 and the TM_2 modes. The wave amplitudes a_2 are now the reflection coefficients while a_0 become the coupling coefficients on the reflected fundamental modes. In contrast with the previous fundamental excitations, the reflection coefficients a_2 approach closely the unit value when the normalized frequency increases.

In the TE case (Fig. 9) its behavior denotes a more important coupling with the evanescent continuous modes rather than with the radiated continuous modes at the discontinuity. A similar behavior is met for the TE_0 magnetic dipole mode of the dielectric rod when it is confined in a resonator. Indeed, closed-form expressions of its resonant frequency can be obtained by assuming an energy storage in the neighborhood of the two interacting discontinuities and small radiation losses [18]. In the TM case the behavior is quite different since a strong coupling with the radiated continuous modes occurs when $k_0 d$ approaches the "cutoff frequency" of the TM_2 incident mode and Fig. 10 shows that this leakage of energy is felt in a large range of variation of the normalized frequency. Note lastly the efficient excitations of the reflected fundamental modes at the discontinuity in Figs. 9 and 10.

IV. Conclusion

In conclusion, a new rigorous analysis of transverse discontinuities in a dielectric slab waveguide has been outlined on the abruptly ended configuration. The key point is the derivation of coupled integral equations on discrete and continuous waves amplitudes of the modal fields at the discontinuity. These coupled integral equations are solved by an iterative procedure namely the Neuman series.

Numerical examples involving various even TE and TM excitations are reported. For more practical structures such as dielectric rods, the analytical description of the discrete and continuous modes spectra differs but the concepts involved remain the same. The rigorous formulation of the resonances of a dielectric cylindrical resonator deserves further attention.

Appendix

Odd TM Excitations in an Abruptly Ended Slab Waveguide

The continuity relation between transverse fields at the interface $z=0$ is quite similar to (1) after a simple interchanging of the subscripts x and y in fields quantities.

The discrete and the continuous transverse modal fields must be necessary modified as it follows. So, for discrete odd TM slab mode in region I, we obtain

$$H_{x,n} = \begin{cases} A_n \cos K_n x, & |x| < d \\ A_n e^{\gamma_n d} \cos K_n d \, e^{-\gamma_n |x|}, & |x| > d \end{cases}$$

$$E_{y.n} = \frac{\beta_n}{\omega \epsilon_0 \epsilon_r(x)} H_{x,n} \tag{A-1}$$

$$\epsilon_r(x) = \begin{cases} \epsilon_r, & |x| < d \\ 1, & |x| > d \end{cases}. \tag{A-2}$$

The transverse wavenumbers K_n and γ_n are now connected by the characteristic equation

$$K_n \tan K_n d = \epsilon_r \gamma_n \tag{A-3}$$

and from the power flow normalization we derived the value of the constant A that is

$$A_n=\sqrt{\frac{2\omega\epsilon_0 P\cdot\gamma_n\cdot\epsilon_r\cdot(\epsilon_r\cdot\gamma_n^2+\beta_n^2)}{\beta_n\left[\omega^2\mu_0\epsilon_0\epsilon_r+\gamma_n d\cdot(\epsilon_r\gamma_n^2+\beta_n^2)\right]}}\ . \quad \text{(A-4)}$$

The continuous odd TM slab modes in region I are expressed as

$$H_y(\rho)=\begin{cases} B_e^r(\rho)\cos\sigma x, & |x|<d \\ B_e^r(\rho)\left[D_e^r(\rho)e^{-i\rho|x|}+D_e^{r*}(\rho)e^{i\rho|x|}\right], & |x|>d \end{cases}$$

$$E_x(\rho)=-\frac{\beta(\rho)}{\omega\epsilon_0\epsilon_r(x)}H_y(\rho) \quad \text{(A-5)}$$

where

$$D_e^r(\rho)=\frac{1}{2}\left[\cos\sigma d-\frac{i}{\epsilon_r}\frac{\sigma}{\rho}\sin\sigma d\right]e^{i\rho d} \quad \text{(A-6)}$$

$$B_e^r(\rho)=\rho\sqrt{\frac{2\omega\epsilon_0 P\epsilon_r}{\Pi|\beta(\rho)|\left(\epsilon_r^2\rho^2\cos^2\sigma d+\sigma^2\sin^2\sigma d\right)}} \quad \text{(A-7)}$$

while in region II that is the free space their expressions are

$$H_y(\rho)=B_e^t(\rho)\cos\rho x$$

$$E_x(\rho)=\frac{\beta(\rho)}{\omega\epsilon_0}B_e^t(\rho)\cos\rho x \quad \text{(A-8)}$$

with

$$B_e^t(\rho)=\sqrt{\frac{2\omega\epsilon_0 P}{\Pi|\beta(\rho)|}}\ . \quad \text{(A-9)}$$

Let $\nu_n(\rho)$ and $\kappa_n(\rho)$ the functions, such that

$$\nu_n(\rho)=\int_0^\infty\frac{H_{y,n}^i H_y^{t*}(\rho)}{\epsilon_r(x)}dx, \qquad n=0,2,4,\cdots \quad \text{(A-10)}$$

$$\kappa_n(\rho)=\int_0^\infty H_{y,n}^i H_y^{t*}(\rho)\,dx, \qquad n=0,2,4,\cdots . \quad \text{(A-11)}$$

Then the system coupled integral equations connecting the waves amplitudes $q_t(\rho)$, $q^r(\rho)$, and a_n that take the place of (2) and (3) are

$$q^t(\rho)=\frac{1}{\omega\epsilon_0 P}\frac{\beta\rho}{\nu_0(\rho)\beta_0+\kappa_0(\rho)\beta(\rho)}\left\{2\beta_0\cdot\nu_0(\rho)\cdot\kappa_0(\rho)\right.$$
$$+\int_0^\infty d\rho'\int_0^\infty q^r(\rho')\left[\beta_0\cdot\nu_0(\rho)\cdot H_y^r(\rho')\right.$$
$$\left.\cdot H_y^{t*}(\rho)-\beta(\rho')\kappa_0(\rho)\cdot\frac{H_y^r(\rho')H_y^{t*}(\rho)}{\epsilon_r(x)}\right]dx$$
$$\left.+\sum\left[\beta_0\cdot\kappa_n(\rho)\cdot\nu_0(\rho)-\beta_n\cdot\nu_n(\rho)\cdot\kappa_0(\rho)\right]a_n\right\},$$
$$n=2,4,\cdots \quad \text{(A-12)}$$

$$\begin{Bmatrix} a_n \\ q^r(\rho)\end{Bmatrix}=\frac{1}{4\omega\epsilon_0 P}\frac{\begin{Bmatrix}-\beta_n\\ |\beta(\rho)|\end{Bmatrix}}{\begin{Bmatrix}\beta_n\\ \beta(\rho)\end{Bmatrix}}$$
$$\cdot\int_0^\infty d\rho'\cdot q^t(\rho')\left[\beta(\rho)\cdot\begin{Bmatrix}\dfrac{H_y^t(\rho')H_y^{r*}(\rho)}{\epsilon_r(x)}\\ \kappa_n(\rho)\end{Bmatrix}\right.$$
$$\left.-\begin{Bmatrix}\beta(\rho) & H_y^t(\rho)H_y^{r*}(\rho)\,dx\\ -\beta_n & \nu_n(\rho)\end{Bmatrix}\right],$$
$$n=0,2,4,\cdots \quad \text{(A-13)}$$

we can also obtained the following integral equation:

$$1=\frac{1}{4\omega\mu_0 P}\int_0^\infty q^t(\rho)\cdot(\beta(\rho)\cdot\kappa_0(\rho)+\beta_0\cdot\nu_0(\rho))\cdot d\rho \quad \text{(A-14)}$$

which appears as useful for test on accuracy in the computational scheme as (14). The power conservation equation of the TM excitations is the same that (10).

ACKNOWLEDGMENT

The authors would like to thank J. Rembowski of the specialized translation service of the Cueep of the Technical University of Lille I for his help during the preparation of the manuscript.

REFERENCES

[1] J. Van Bladel, "On the resonances of a dielectric resonator of very high permittivity," *IEEE Trans. Microwave Theory Tech.*, vol. MTT-23, pp. 199–208, Feb. 1975.
[2] P. J. Clarricoats and K. R. Slinn, "Numerical solution of waveguide discontinuity problems," *Proc. Inst. Elec. Eng.*, vol. 114, pp. 878–886, July 1967.
[3] D. Marcuse, "Radiation losses of tapered dielectric slab waveguides," *Bell Syst. Tech. J.*, vol. 49, no. 2, pp. 273–290, Feb. 1970.
[4] L. Lewin, "A method for the calculation of the radiation pattern and mode conversion properties of a solid state heterojunction laser," *IEEE Trans. Microwave Theory Tech.*, vol. MTT-23, pp. 576–585, July 1975.
[5] S. Mahmoud and J. Beal, "Scattering of surface waves at a dielectric discontinuity on a planar waveguide," *IEEE Trans. Microwave Theory Tech.*, vol. MTT-23, pp. 193–198, Feb. 1975.
[6] K. Morishita, S. E. Inagaki, and N. Kumagai, "Analysis of discontinuities in dielectric waveguides by means of the least squares boundary residual method," *IEEE Trans. Microwave Theory Tech.*, vol. MTT-27, pp. 310–315, Apr. 1979.
[7] T. E. Rozzi, "Rigorous analysis of the step discontinuity in a planar dielectric waveguide," *IEEE Trans. Microwave Theory Tech.*, vol. MTT-26, pp. 738–746, Oct. 1978.
[8] R. Collin, *Field Theory of Guided Waves*. New York: McGraw-Hill, 1960, ch. 8.
[9] Ph. Gelin, M. Petenzi, and J. Citerne, "New rigorous analysis of the step discontinuity in a slab dielectric waveguide," *Electron Lett.*, vol. 15, no. 12, pp. 355–365, June 1979.
[10] H. Kressel and J. K. Butler, *Semiconductor Lasers and Heterojunction LEDs*. New York: Academic, ch. 5.
[11] R. E. Collin and F. Zucker, *Antenna Theory*. New York: McGraw-Hill, 1969.

[12] C. Angulo, "Diffraction of surface waves by a semi infinite dielectric slab," *IRE Trans. Antennas Propagat.*, vol. AP-5, pp. 100–109, Jan. 1957.
[13] G. A. Hockham and A. B. Sharpe, "Dielectric waveguide discontinuities," *Electron. Lett.*, vol. 8, pp. 230–231, May 1972.
[14] T. Ikegami, "Reflectivity of mode at facet and oscillation mode in double heterojunction injection lasers," *IEEE J. Quantum Electron.*, vol. QE-6, pp. 470–476, June 1972.
[15] F. K. Reinhart, I. Hayashi, and M. Panish, "Mode reflectivity and waveguide properties of double heterostructure injection lasers," *J. Appl. Phys.*, vol. 42, no. 11, pp. 4466–4479, Oct. 1971.
[16] T. E. Rozzi and G. H. in't Veld, "Variational treatment of the diffraction at the facet of d.h. lasers and dielectric millimeter wave antennas," *IEEE Trans. Microwave Theory Tech.*, pp. 61–73, Feb. 1980.
[17] B. Rulf, "Discontinuity radiation in surface waveguides," *J. Opt. Soc. Amer.*, vol. 65, no. 11, pp. 1248–1252, Nov. 1975.
[18] H. Y. Yee, "National resonant frequencies of microwave dielectric resonators," *IEEE Trans. Microwave Theory Tech.*, vol. MTT-13, p. 256, Mar. 1965.
[19] C. T. Baker, *The Numerical Treatment of Integral Equation*. Oxford, England: Clarendon Press, pp. 34–37.

An Analysis of Log Periodic Antenna with Printed Dipoles

ALAKANANDA PAUL, MEMBER, IEEE, AND INDERJEET GUPTA

Abstract—**An analysis of Log Periodic Antenna with Printed Dipoles is presented here. In this analysis, the wave equation for Hertz potential is solved in Cartesian coordinates applying the boundary conditions of a flat strip dipole. Using this model, the input currents to the antenna elements, the current distribution of the antenna elements, and the radiation pattern are computed. The computed results are compared with experimental results.**

I. Introduction

IN RECENT years frequency independent antennas [1] have gained significant importance. The Log Periodic Dipole Array (LPDA) is an important type of frequency independent antenna and was invented by Isbell [2] at the University of Illinois in 1958.

Several theories based on the transmission line approach have been put forth for the analysis of LPDA [3], [4], [5]. Wolter [6] derived a theory of Log Periodic Dipole Antenna as a solution of the antenna boundary value problem. He calculated the current distribution on antenna elements by solving the wave equation for Hertz potential in cylindrical coordinates, satisfying the appropriate boundary conditions.

At microwave frequencies, wire dipoles may be bent due to rough handling causing asymmetries in the structure, which, in turn result in back radiation and side lobes [7]. Therefore, it is better to replace the wire antenna by printed dipole which is more rugged and can be easily fabricated.

In this paper, a mathematical model for the analysis of LP array using printed dipole is developed following Wolter's method [6]. However, in this case, the wave equation for Hertz potential is solved in rectangular coordinates satisfying the boundary conditions of a flat strip dipole.

II. Analysis

The antenna consists of N parallel flat strip dipoles. The antenna lies in the x–y plane of the rectangular coordinate system as shown in Fig. 1. The details of the nth element are shown in Fig. 2 and the dimensions of the test array are given in Table I. The elements are fed by a symmetrical transmission line with the characteristic impedance z_0. The two conductors of the transmission line are separated by a dielectric sheet of thickness t. An extra phase shift of 180° is introduced by switching the connection of the adjacent elements.

In the following analysis the dipole elements are assumed infinitely thin and perfectly conducting for the sake of simplicity. If t is infinitesimally small, the two strips of elements can be considered to be at $z=0$. Taking the time variation as $\exp(j\omega t)$ the wave equation for Hertzian vector will reduce to

$$\Delta\pi_n + K_0^2\pi_n = 0 \tag{1}$$

where K_0 is the wavenumber in free space. π_n will have only y component due to the choice of coordinate system. Since each element is symmetrical in x, y, and z about its

Manuscript received August 23, 1979; revised September 19, 1980.

A. Paul is with the Electrical Engineering Department, Northeastern University, Boston, MA 02115, on leave from the Department of Electrical Engineering, Indian Institute of Technology, Kanpur 208016, India.
I. Gupta is with with the Department of Electrical Engineering, Ohio State University, Columbus, OH 43210.

0018-9480/81/0200-0114$00.75